Altered expression profile of glycolytic enzymes during testicular ischemia reperfusion injury is associated with the p53/TIGAR pathway: Effect of fructose 1,6-bisphosphate

May Al-Maghrebi [Corresp., 1] , Waleed M Renno [2]

[1] Faculty of Medicine - Department of Biochemistry, Kuwait University, Safat, Kuwait

[2] Faculty of Medicine - Department of Anatomy, Kuwait University, Safat, Kuwait, Kuwait

Corresponding Author: May Al-Maghrebi
Email address: malmaghrebi@hsc.edu.kw

Background: Testicular ischemia reperfusion injury (tIRI) is considered the mechanism underlying the pathology of testicular torsion and detorsion. Left untreated, tIRI can induce testis dysfunction, damage to spermatogenesis and possible infertility. In this study, we aimed to assess the activities and expression of glycolytic enzymes (GEs) in the testis and their possible modulation during tIRI. The effect of fructose 1,6-bisphosphate (FBP), a glycolytic intermediate, on tIRI was also investigated.

Methods: Male Sprague-Dawley rats were divided into three groups: sham, unilateral tIRI, and tIRI + FBP (2 mg/kg). tIRI was induced by occlusion of the testicular artery for 1 h followed by 4 h of reperfusion. FBP was injected peritoneally 30 min prior to reperfusion. Histological and biochemical analyses were used to assess damage to spermatogenesis, activities of major GEs, and energy and oxidative stress markers. The relative mRNA expression of GEs was evaluated by real-time PCR. ELISA and immunohistochemistry were used to evaluate the expression of p53 and TP53-induced glycolysis and apoptosis regulator (TIGAR).

Results: Histological analysis revealed tIRI-induced spermatogenic damage as represented by a significant decrease in the Johnsen biopsy score. In addition, tIRI reduced the activities of hexokinase 1, phosphofructokinase-1, glyceraldehyde 3-phosphate dehydrogenase, and lactate dehydrogenase C. However, mRNA expression downregulation was detected only for hexokinase 1, phosphoglycerate kinase 2, and lactate dehydrogenase C. ATP and NADPH depletion was also induced by tIRI and was accompanied by an increased Malondialdehyde concentration, reduced glutathione level, and reduced superoxide dismutase and catalase enzyme activities. The immunoexpression of p53 and TIGAR was markedly increased after tIRI. The above tIRI-induced alterations were attenuated by FBP treatment.

Discussion: Our findings indicate that tIRI-induced spermatogenic damage is associated with dysregulation of GE activity and gene expression, which were associated with activation of the TIGAR/p53 pathway. FBP treatment had a beneficial effect on alleviating the damaging effects of tIRI. This study further emphasizes the importance of metabolic regulation for proper spermatogenesis.

1 The altered expression profile of glycolytic enzymes during testicular ischemia reperfusion

2 injury is associated with the p53/TIGAR pathway: Effect of fructose 1,6-bisphosphate

5 May Al-Maghrebi[1]*, Waleed M. Renno[2]

8 Departments of [1]Biochemistry and [2]Anatomy, Faculty of Medicine-Kuwait University, Jabriyah,

9 Kuwait

12 *Corresponding Author

14 ***Address for correspondence***

15 Dr. May Al-Maghrebi, PhD

16 Department of Biochemistry

17 Faculty of Medicine, Kuwait University

18 P.O. Box: 24923, Safat13110, Kuwait

19 Tel: 965 24636447   Fax: 965 25338908

20 E-mail address: malmaghrebi@hsc.edu.kw

24 **Running Title:** Regulation of glycolytic enzymes in testicular ischemia reperfusion injury

26 **ABSTRACT**

27 **Background:** Testicular ischemia reperfusion injury (tIRI) is considered the mechanism

28 underlying the pathology of testicular torsion and detorsion. Left untreated, tIRI can induce testis

29 dysfunction, damage to spermatogenesis and possible infertility. In this study, we aimed to assess

30 the activities and expression of glycolytic enzymes (GEs) in the testis and their possible

31 modulation during tIRI. The effect of fructose 1,6-bisphosphate (FBP), a glycolytic intermediate,

32 on tIRI was also investigated. **Methods:** Male Sprague-Dawley rats were divided into three

33 groups: sham, unilateral tIRI, and tIRI + FBP (2 mg/kg). tIRI was induced by occlusion of the

34 testicular artery for 1 h followed by 4 h of reperfusion. FBP was injected peritoneally 30 min

35 prior to reperfusion. Histological and biochemical analyses were used to assess damage to

36 spermatogenesis, activities of major GEs, and energy and oxidative stress markers. The relative

37 mRNA expression of GEs was evaluated by real-time PCR. ELISA and immunohistochemistry

38 were used to evaluate the expression of p53 and TP53-induced glycolysis and apoptosis regulator

39 (TIGAR). **Results:** Histological analysis revealed tIRI-induced spermatogenic damage as

40 represented by a significant decrease in the Johnsen biopsy score. In addition, tIRI reduced the

41 activities of hexokinase 1, phosphofructokinase-1, glyceraldehyde 3-phosphate dehydrogenase,

42 and lactate dehydrogenase C. However, mRNA expression downregulation was detected only for

43 hexokinase 1, phosphoglycerate kinase 2, and lactate dehydrogenase C. ATP and NADPH

44 depletion was also induced by tIRI and was accompanied by an increased Malondialdehyde

45 concentration, reduced glutathione level, and reduced superoxide dismutase and catalase enzyme

46   activities. The immunoexpression of p53 and TIGAR was markedly increased after tIRI. The

47   above tIRI-induced alterations were attenuated by FBP treatment.

48   **Discussion:** Our findings indicate that tIRI-induced spermatogenic damage is associated with

49   dysregulation of GE activity and gene expression, which were associated with activation of the

50   TIGAR/p53 pathway. FBP treatment had a beneficial effect on alleviating the damaging effects

51   of tIRI. This study further emphasizes the importance of metabolic regulation for proper

52   spermatogenesis.

53

54   **Keywords:** Testicular ischemia reperfusion injury, Glycolytic enzymes, Fructose 1,6-

55   bisphosphate, Gene expression regulation, Apoptosis, Oxidative stress.

56

57

58

59

60

61

62

63

64

65

66

67

68

69

70

71

72

73

74

INTRODUCTION

Testicular ischemia reperfusion injury (tIRI) represents the events that occur during testicular

torsion and detorsion (TDD) (Filho et al., 2004). Prompt surgical intervention to counter rotation

of the spermatic cord is necessary to relieve the acute ischemic episode. However, it has been

established that tIRI induces the generation of reactive oxygen species (ROS) that trigger an

array of signaling molecules, causing progressive damage to the structure and function of the

testis (Filho et al., 2004; Antonuccio et al., 2006; Minutoli et al., 2012). A potentially negative

outcome of tIRI is the increased risk of impaired spermatogenesis and reduced male fertility.

Throughout spermatogenesis, germ cells have unique metabolic needs and utilize different

metabolic pathways for energy production to ensure proper development (Boussouar &

Benahmed 2004; Rato et al., 2012). Therefore, the maintenance of metabolic requirements

necessitates the cooperation of germ cells with Sertoli cells (SCs) to ensure proper

spermatogenesis (Alves et al., 2014). Spermatogenesis is under hormonal control that involves

SCs; thus, it can be inferred that the glycolytic metabolism of SCs might be affected by this

hormonal signaling (Alves et al., 2013). Moreover, the metabolic status of the reproductive

system is vital to maintain germ cell energy demands and survival. Several studies have reported

on the implications of metabolic defects on male infertility in patients with Klinefelter syndrome,

92   diabetes mellitus, or obesity (Alves et al., 2016a; Alves et al., 2015; Martins 2015; Rato et al.,

93   2015).

94   During spermatogenesis, germ cells interchangeably utilize lactate and glucose as energy

95   sources. Spermatids predominantly use the TCA cycle for energy production, whereas

96   spermatogonia depend on glycolysis for energy production (Robinson & Fritz, 1981; Riera et al.,

97   2002). SCs act as lactate producers in the testis by sustaining a high glycolytic flux, thus

98   exhibiting Warburg-like metabolic behavior (Oliveira et al., 2015). This is very important for

99   supporting the energetic needs of developing germ cells. Most of the glucose is converted to

100   lactate, which is then converted to pyruvate by the enzyme lactate dehydrogenase C (LDHC).

101   Interestingly, approximately 25% of the produced pyruvate becomes oxidized during the TCA

102   cycle. This reaction is coupled with NADPH production, an indicator of the pentose phosphate

103   pathway (PPP). Surplus glucose undergoes glycolysis to produce pyruvate that enters the

104   mitochondria and becomes oxidized and decarboxylated by pyruvate dehydrogenase to form

105   acetyl CoA that enters the TCA cycle. During this process, ATP is formed by ADP

106   phosphorylation via the electron transport chain (Rato et al., 2002). Several glycolytic enzymes

107   (GEs), including hexokinase isoenzyme 1 (HK1S), glucose-6-phosphate isomerase (GPI),

108   phosphoglycerate kinase (PGK2), sperm-specific glyceraldehyde 3-phosphate (GAPDHS), and

109   pyruvate kinase (PKS), have been identified and reported to play a key role in regulating

110   glycolysis in germ cells(Gupta, 2013). An interesting glycolysis intermediate, fructose-1,6-

111   bisphosphate (FBP), has been shown to exert protective effects in several models of ischemia

112   and hypoxia (Didlake et al., 1989; Farias et al., 1990; Karaca et al., 2002). It was also suggested

113   that FBP can activate the PPP for anaerobic ATP production (Kelleher et al., 1995; Espanol et

114   al., 1998). The PPP is involved in the regulation of cellular redox via NADPH supplementation.

115 NADPH is considered a regulator of cellular redox potential by preserving cellular levels of

116 glutathione and catalase (Ben-Yosef, Boxer, & Ross 1996; Salvemini et al., 1999). Similarly,

117 FBP was found to maintain cellular levels of glutathione and catalase in addition to upregulating

118 the activity of glucose-6-phosphate dehydrogenase, the rate-limiting enzyme of PPP. Therefore,

119 it is highly likely that FBP suppresses oxidative stress through PPP activation (Ahn et al., 2002).

120 In the present study, we evaluated the mRNA expression and activity of the major GEs

121 required for energy production in the testis during tIRI. In parallel, testicular oxidative status and

122 germ cell apoptosis were also assessed. Due to its reported protective and antioxidant effects, we

123 investigated the effects of the exogenous administration of FBP on spermatogenesis, expression

124 of GEs, and energy production in the testis. The effects of tIRI-induced ROS on the expression

125 of p53 and its downstream transcriptional target TP53-induced glycolysis and apoptosis regulator

126 (TIGAR) were also studied.

127

128 **MATERIALS AND METHODS**

129 **Ethics Statement**

130 The animal experimental protocol and procedures used in this study complied with the guidelines

131 of the ethics committee on animal research at Kuwait University. The ethical use of animals at

132 Kuwait University is in accordance with the guidelines of the International Council for

133 Laboratory Animal Sciences (ICLAS). Male adult Sprague-Dawley rats (Charles River,

134 Waltham, MA, USA) were acclimated to standard laboratory conditions of a 12-h light/12-h dark

135 cycle at 25°C, and were fed a standard diet and tap water *ad libitum*.

136

137 **Surgical Procedure**

138   The rats (n = 18, 200-250 g, 8 weeks old) were divided randomly into three groups of six rats

139   each. The three groups were: sham, tIRI, and tIRI + FBP. The surgical procedure has been

140   described previously (Al-Maghrebi, Renno & Al-Ajmi, 2012). Briefly, all rats were anesthetized

141   with 50 mg/kg ketamine (Tekam, Hikma Pharmaceuticals, Amman, Jordan) and 2 mg/kg

142   xylazine (Rompun, Bayer GmbH, Leverkusen, Germany). The incision area was clean-shaven

143   and disinfected with betadine. Sham rats underwent a standard ilioinguinal incision at the left

144   side, and the left testis was exposed for 60 min before placing it again into the scrotal sac

145   followed by incision suturing. Sham animals were sacrificed after 4 h. The rats subjected to tIRI

146   underwent a unilateral ischemic injury by occluding the left testicular artery with a non-traumatic

147   microvascular clamp (700 g of pressure) (Cat. No. RS-7440; Roboz Surgical Instruments Co.,

148   Gaithersburg, MD, USA) to cut off the blood supply to the testes for 1 h. Thirty minutes prior to

149   testis reperfusion, the rats received an intraperitoneal injection (i.p.) injection of 300 µl of saline

150   (vehicle). Blood flow was resumed after 1 h of ischemia by clamp removal, and testis

151   reperfusion was allowed for 4 h before animal sacrifice. A similar procedure was followed with

152   the third group that underwent tIRI + FBP, in which saline was substituted with a dose of 2 g/kg

153   FBP. FBP (Cat. No. F6803; Sigma-Aldrich, St. Louis, MO, USA) was administered as an i.p. of

154   2 mg/kg 30 min prior to reperfusion. The selected dose and method of delivery were based on

155   prior studies (Zhou J et al., 2014; Palanas et al., 1993). Zhou and colleagues, 2014, showed that

156   an i.p. FBP dose of 500 or 1,000 mg/kg provided neuroprotection in immature rats suffering

157   from repeated febrile convulsions. Palanas and colleagues, 1993, demonstrated that in contrast to

158   lower i.p. doses of FBP (0.5 or 1 g/kg) or the orally administered dose of 0.5 g/kg, an i.p.

159   injection of 2 g/kg FBP had the highest protective action (80%) within 1 h of administration and

160   persisted for 5 h (Palanas et al., 1993). Furthermore, albino Swiss mice showed no toxicity

161   symptoms after an i.p. administration of 800 mg/kg FBP. The availability of FBP for 5 h and low

162   toxicity are important to evaluate its protective effects in our experimental design. For all three

163   animal groups, the right contralateral testes were used as a positive internal control.

164

Histological Examination

165

166   The harvested testes were immediately immersed in Bouin's fixative for 24 h, washed with PBS,

167   and embedded in paraffin. Hematoxylin and eosin (H&E) staining was used to stain 4-μm tissue

168   sections. Spermatogenesis was evaluated by measuring the tissue biopsy score (TBS) using the

169   Johnson scoring system, which is based on rating germ cell maturation in each seminiferous

170   tubule using a score of 1-10 (Johnsen, 1970). In a blinded manner, 4 slides from each testis (6

171   contralateral and 6 ipsilateral testes) were used for scoring.

172

Detection of Apoptosis

173

174   Dewaxed and rehydrated 4-μm tissue sections were treated with proteinase K followed by

175   incubation with the TUNEL reaction mixture at 37°C and then were mounted with DAPI.

176   Staining of non-apoptotic free DNA 3' ends was eliminated by adjusting the manufacturer's

177   protocol (Cat. No. 11684795910; Roche-Diagnostics, Mannheim, Germany). TUNEL-stained

178   nuclei were analyzed using the LSM 700 confocal laser scanning microscope (Carl Zeiss Micro-

179   Imaging, München, Germany). TUNEL-stained nuclei were scored using 100 random

180   seminiferous tubules from 2 slides/testis/rat. Images were acquired at 400× and 100×

181   magnification for counting and presentation purposes, respectively. The investigator was blinded

182   to the experimental group identity during the scoring process, and the data are presented as the

183   mean ± SD.

184

185 **Immunohistochemistry**

186 Each testis paraffin block was cut into 4-mm sections on silane-coated slides. The avidin-biotin

187 complex method was used for p53 and TIGAR immunohistochemical staining. Tissues were

188 rehydrated in a graded alcohol series followed by microwave retrieval using citrate buffer (0.01

189 M, pH 6). The tissues were then treated for 30 min in 3% H_2O_2, washed in PBS and blocked in

190 blocking solution (Cat. No. 85-8943; Invitrogen, Frederick, MD, USA). The processed slides

191 were incubated overnight with primary antibodies (1:100 dilution) for p53 (Cat. No. (DO-1) sc-

192 126; Santa Cruz Biotechnology, Santa Cruz, CA, USA) and for TIGAR (Cat. No. (Y-20) sc-

193 68239; Santa Cruz Biotechnology, Santa Cruz, CA, USA). The slides were then washed and

194 treated with a Histostain-*Plus* IHC Kit, HRP, and broad-spectrum secondary antibody

195 (60:40) (Cat. No. 85-8943; Thermo Fisher Scientific, Waltham, MA, USA) for 30 min at room

196 temperature. The slides were then washed three times in PBS and treated with HRP-Streptavidin

197 (Cat. No. N200; Thermo Fisher Scientific, Waltham, MA, USA) for 30 min at room temperature.

198 Color development was then carried out using the Impact DAB kit (Cat. No. SK-4105; Vector

199 Labs, Burlingame, CA, USA) for 30 sec or until the desired brown color was obtained as seen

200 under the microscope. The slides were then washed in distilled water and counterstained with

201 hematoxylin for 5 min, followed by bluing under tap water for 5 min. The slides were dehydrated

202 through a graded series of alcohol from 50% to absolute alcohol and then were cleared in xylene.

203 Finally, a coverslip was mounted on top of the tissue sections using histology DPX mountant.

204 The mean immunolabeling concentration was assessed by measuring the color intensity (Sum

205 (Area) (pixel²) using Cell Sens Dimension Software (Olympus DP 71 camera) in the three

206 experimental groups. Slide analysis was performed in a blinded manner.

207

208 **RT and Real-time PCR**

209 Total RNA was purified from frozen testicular tissue samples using TRIzol (Invitrogen, USA)

210 following the manufacturer's instructions. Total RNA was reverse transcribed into

211 complementary DNA (cDNA) using a high-capacity cDNA reverse transcription kit (RT)

212 (Thermo Fisher Scientific, Waltham, MA, USA). The reaction mixtures included 20 U of reverse

213 transcriptase, 10 µl of first-strand buffer, random primers, 0.5 mM dNTP mix and 10 mM DDT.

214 RT reactions were carried out at 55°C for 50 min. The gene expression levels of the following

215 GEs were quantitated using real-time PCR: hexokinase (*hk1*, Cat. No. Rn00562436_m1),

216 glucose-6-phosphate isomerase (*gpi*, Cat. No. Rn01475756_m1), 6-phosphofructokinase 1 (*pfk*,

217 custom made), glyceraldehyde 3-phosphate dehydrogenase Sperm (*gapdhs*, Cat. No.

218 Rn01476455_m1), phosphoglycerate kinase 2 (*pgk2*, Cat. No. Rn01511987_s1), and lactate

219 dehydrogenase C (*ldhc*, Cat. No. Rn00568562_m1). The mRNA levels for the p53 upregulated

220 modulator of apoptosis (*puma*, Cat. No. Rn00597992_m1) and survivin (*birc5*, Cat. No.

221 Rn00574012_m1) were also measured. Gene-specific Taqman assays were mixed with

222 TaqMan® universal PCR master mix (Thermo Fisher Scientific, Waltham, MA, USA) in a 96-

223 well plate. The reaction conditions recommended by the manufacturer were used in compliance

224 with the ABI Prism 7000 SD system (Thermo Fisher Scientific, Waltham, MA, USA). The

225 relative mRNA expression was calculated using the $2^{-\Delta\Delta CT}$ method (Livak & Schmittgen, 2001).

226 A rat β-actin (*actb*, Cat. No. Rn00667869_m1)-specific Taqman assay was used as an

227 endogenous control.

228

229 **Protein Purification**

230   Total protein crude extracts were prepared from harvested testicular tissue. The tissues were

231   homogenized in a lysis buffer (20 mM Tris, 150 mM NaCl, 10 mM Na_2EDTA, 10 mM EGTA,

232   1% Triton X-100, 1 mM Na_3VO_4, 25 mM NaF, 1 µg/ml leupeptin, and 1 mM PMSF) using a

233   tissue homogenizer. The protein concentrations were measured using the Bradford assay (Bio-

234   Rad, Hercules, CA, USA) and bovine serum albumin as the standard.

235

236   **Biochemical Assays**

237   Colorimetric assays were purchased from Sigma-Aldrich (St. Louis, MO, USA) to measure the

238   enzymatic activities of HK1 (Cat. No. MAK091), GPI (Cat. No. MAK103), PFK1 (Cat. No.

239   MAK093), GAPDH (Cat. No. MAK277), PGK2 (Cat. No. P7634), and LDHC (Cat. No.

240   MAK066) following the manufacturer's protocols. The protein expression of total p53 and p-p53

241   (ser 15) was measured using an ELISA kit (Cat. No. PEL-P53-S15-T-1; RayBiotech, Inc.,

242   Norcross, GA, USA) following the manufacturer's protocol. The levels of ATP (Cat. No.

243   MAK190) and NADPH (Cat. No. MAK038) were measured using their respective colorimetric

244   assays according to the manufacturer's recommendations (Sigma-Aldrich, St. Louis, MO, USA).

245   The testicular levels of glutathione (GSH, Cat. No. CS0260), malondialdehyde (MDA, Cat. No.

246   MAK085) and the antioxidant enzymes superoxide dismutase (SOD, Cat. No. 19160) and

247   catalase (CAT, Cat. No. CAT100) were determined using their respective colorimetric assays

248   (Sigma-Aldrich, St. Louis, MO, USA) following the manufacturer's protocol.

249

250   **Statistical Analysis**

251   Statistical analysis for the obtained data was performed using GraphPad Prism (v 6.0). All of the

252   data are presented as the mean ± standard deviation (SD). Grubb's test and/or ROUT test were

253   used to eliminate any outliers from the normal data distribution. Multiple group comparisons

254   were performed using one-way analysis of variance (ANOVA) followed by the Holm-Sidak

255   multiple comparisons test for the comparison of mean values. Statistical significance was

256   accepted as $p < 0.05$.

257

258   **RESULTS**

259   **Testicular spermatogenesis**

260   Figure 1 shows H&E testicular sections from the sham, tIRI, and FBP-treated groups. In contrast

261   to the normal histological appearance of testicular tissue in the sham and FBP-treated groups, the

262   ipsilateral testes in the tIRI group showed seminiferous tubular atrophy, disruption of germ cell

263   layers, and spermatogenic arrest. Compared with sham, the mean TBS in the ipsilateral testes

264   from the tIRI group was significantly lower (9.33 ± 1.03 *vs.* 5.67 ± 0.52, $p < 0.0001$), which was

265   normalized after FBP treatment (7.67 ± 0.52, *vs.* 5.67 ± 0.52, $p = 0.0002$). The contralateral

266   testes revealed no significant differences in testis histology or TBS among the three experimental

267   groups.

268

269

270

271   **mRNA expression of glycolytic enzymes**

272   The relative mRNA expression was obtained and calculated for all of the evaluated genes (Table

273   1). The mRNA expression for *gpi* and *pgk2* showed no significant changes among the three

274   experimental groups. However, significant downregulation of the mRNA expression of *hk1* (0.76

275   ± 0.46 *vs.* 1.00 ± 0.26, $p < 0.05$), *pfk* (0.66 ± 0.39 *vs.* 1.00 ± 0.27, $p < 0.05$), *gapdhs* (0.73 ± 0.39

276   *vs.* 1.00 ± 0.32, $p < 0.05$), and *ldhc* (0.76 ± 0.46 *vs.* 1.00 ± 0.26, $p < 0.05$) was calculated in the

277   tIRI group compared with sham levels and was restored to almost sham levels in the FBP-treated

278   group. The contralateral testes revealed no significant differences in mRNA expression among

279   the three experimental groups.

280

281   **Glycolytic enzyme activities**

282   The enzymatic activities of HK1 (1.11 ± 0.27 *vs.* 2.08 ± 0.30, $p = 0.0034$), PFK1 (0.78 ± 0.10 *vs.*

283   1.33 ± 0.24, $p = 0.0016$), GAPDHS (1.05 ± 0.21 *vs.* 1.49 ± 0.14, $p = 0.0016$) and LDHC ($1.07 \pm$

284   0.17 *vs.* 2.02 ± 0.41, $p < 0.0001$) were significantly decreased as a result of tIRI compared with

285   sham levels (Table 2). These activities were significantly increased in the FBP-treated group

286   compared with that in the tIRI group (HK1: 1.87 ± 0.38, $p = 0.0260$; PFK1: 1.30 ± 0.17, $p =$

287   0.0029; GAPDHS: 1.46 ± 0.28, $p = 0.0040$; LDHC: 1.78 ± 0.19, $p = 0.0017$). Although there

288   were notable decreases in the activities of GPI and PGK2 in the tIRI group, the decreases were

289   not significantly different from those of the sham or FBP-treated group. The contralateral testes

290   revealed no significant difference in enzymatic activities among the three experimental groups.

291

292   **Testicular levels of ATP and NADPH**

293   The levels of ATP and NADPH were evaluated in the three experimental groups (Figure 2). In

294   the tIRI group, testicular tissue showed significantly reduced ATP levels (0.41 ± 0.08 *vs.* $0.59 \pm$

295   0.05, $p = 0.0087$) and NADPH levels (1.75 ± 0.36 *vs.* 2.88 ± 0.30, $p = 0.0004$) compared with

296   those in the sham group. FBP-treated rats exhibited sham-like levels of ATP (0.57 ± 0.12 *vs.*

297   0.41 ± 0.08, $p = 0.0286$) and NADPH (2.53 ± 0.32 *vs.* 1.75 ± 0.36, $p = 0.0168$) compared with

298   tIRI. The contralateral testes revealed no significant differences in the evaluated parameters

299   among the three experimental groups.

300

301 **Testicular oxidative stress**

302 In the tIRI group, significantly low GSH (0.33 ± 0.03 *vs.* 0.25 ± 0.04, $p = 0.0002$) and high MDA

303 levels (1.68 ± 0.35 *vs.* 1.05 ± 0.20, $p < 0.0001$) were accompanied by decreased activities of

304 CAT (82.55 ± 8.52 *vs.* 95.32 ± 3.91, $p = 0.0002$) and SOD (81.23 ± 0.95 *vs.* 95.67 ± 3.59, $p <$

305 0.0001) compared with sham (Table 3). FBP treatment reduced testicular oxidative stress as

306 indicated by normalized levels of GSH (0.24 ± 0.03, $p = 0.0002$), MDA (1.04 ± 0.25, $p <$

307 0.0001), and CAT (94.75 ± 4.10, $p = 0.0003$) and SOD (92.62 ± 1.87, $p = 0.0004$) activities. The

308 contralateral testes showed no significant changes in these parameters.

309

310 **Germ cell apoptosis and p53/TIGAR signaling**

311 As shown in Figure 3, ROS-induced DNA damage is clearly visible in the ipsilateral testes

312 subjected to tIRI compared with the sham group (38.67 ± 8.98 *vs.* 0.83 ± 0.75, $p < 0.0001$); this

313 damage was prevented by FBP treatment (9.83 ± 4.62 *vs.* 38.67 ± 8.98, $p < 0.0001$). As shown in

314 Figure 4, DNA damage was accompanied by increased p53 phosphorylation (ser 15) (1.47 ± 0.25

315 *vs.* 0.90 ± 0.11, $p < 0.0001$), upregulated PUMA mRNA expression f (1.71 ± 0.28 *vs.* $1.00 \pm$

316 0.06, $p < 0.05$), and downregulated survivin mRNA expression (0.66 ± 0.15 *vs.* 1.00 ± 0.16, $p <$

317 0.05) in the tIRI group compared with the sham group. Phosphorylation of p53 and the mRNA

318 expression of PUMA and survivin reverted to sham levels in the FBP-treated group [0.96 ± 0.21

319 ($p < 0.0001$), 1.10 ± 0.15 ($p < 0.05$), and 1.14 ± 0.14 ($p < 0.05$), respectively]. This result was

320 also associated with significant increases in the immunostaining of both p53 and TIGAR in tIRI-

321 subjected testes compared with the sham group [p53: $44{,}511 \pm 14{,}731$ *vs.* $1{,}053 \pm 337$, $p <$

322 0.0001; TIGAR: $223{,}212 \pm 61{,}975$ *vs.* $42{,}743 \pm 22{,}900$, $p < 0.0001$] (Figure 5). FBP treatment

323   significantly reduced the immunostaining of both proteins [p53: 5,757 ± 3,223 *vs.* 44,511 ±

324   14,731, $p < 0.0001$; TIGAR: 95,124 ± 48,736 *vs.* 223,212 ± 61,975, $p < 0.0001$].

325

326   **DISCUSSION**

327   Testicular IRI is characterized by reduced spermatogenesis, which could affect testicular

328   function in supporting male fertility. The regulation of carbohydrate metabolism and energy

329   production is important in testicular cells to maintain proper spermatogenesis (Rato et al., 2012).

330   Such processes are carried out through unique metabolic cooperation between somatic SCs and

331   developing germ cells (Alves et al., 2014). Here, we tested the hypothesis that tIRI would affect

332   the metabolic profile of the testis.

333   Glycolysis can be divided into two distinct stages: an energy-consuming stage to produce FBP

334   from glucose, and a second stage comprising energy production via the degradation of FBP to

335   pyruvate (Berg, Tymoczko, & Stryer, 2002). Although SCs and germ cells express all of the

336   enzymes of the glycolytic pathway, germ cells predominantly use the lactate produced by SCs

337   for energy production (Oliveira et al., 2015; Boussouar and Benahmed, 2004). Our data indicate

338   that the transcriptional deregulation of key regulatory GEs from the two glycolytic stages was

339   coupled with respective reduced enzymatic activities, and both were associated with impaired

340   spermatogenesis, increased oxidative stress and germ cell apoptosis. For germ cells, glycolysis is

341   the major source of ATP required for sperm motility, capacitation, and fertilization (Miki, 2007;

342   Mukai and Okuno, 2004; Travis et al., 2004; Williams and Ford, 2001). This result was

343   supported by the localization of the major glycolytic enzymes HK1S, PFK, GAPDHS and LDHC

344   as a unique cluster in the fibrous sheath of the flagellum and in close proximity to the dynein

345   ATPase activity that generates the flagellar beat (Krisfalusi et al., 2006; Nakamura, Mori and

346   Eddy, 2010; Tanii et al., 2007). The importance of their role in supporting sperm bioenergetics

347   and function was further realized in knockout mice for GAPDHS^{-/-} (Miki et al., 2004) and PGK2^{-/-}

348   (Danshina et al., 2010), which showed severely impaired fertility with glycolysis inhibition.

349   Although spermatogenesis appeared normal in LDHC^{-/-} mice (Odet et al., 2013), the sperm

350   fertilization capacity was greatly compromised due to the inability to metabolize lactate for

351   energy production. In addition, immotile sperms had reduced PFK activity compared with motile

352   sperms (Kamp et al., 2007). Furthermore, metal-treated human ejaculates were found to exhibit

353   dose- and time-dependent effects on sperm motility due to the inhibition of GEs such as glucose-

354   6-phosphatase, fructose 1,6-diphosphatase, glucose-6-phosphate isomerase, and lactic

355   dehydrogenase (Kanwar et al., 1988). It was also suggested that the depletion of lactate levels in

356   the testicular tissues of patients with Klinefelter syndrome, a common genetic cause of human

357   infertility, was due to underlying alterations in the testicular metabolism supported by SCs

358   (Alves et al., 2016a). Similarly, compromised levels of testicular lactate content were observed

359   in type I diabetic men and were attributed to alterations in glycolysis-related transporters and

360   enzymes and structural SC deformities, which might be related to impotency problems (Alves et

361   al., 2015). Obesity is another metabolic disease that provides an immediate link between male

362   infertility and deregulated metabolism (Alves et al., 2016b; Katib, 2015; Rato et al., 2014).

363   Impaired sperm quality was associated with defects in energy metabolic pathways in rats fed a

364   high-fat diet (Ferramosca et al., 2016; Rato et al., 2013). Collectively, these data strongly suggest

365   that the impairment of testicular glycolysis due to the deregulated expression and activity of GEs

366   in testicular somatic or germ cells would compromise testicular function and could increase the

367   risk of male infertility.

368   Regular and continuous oxygen supply to the testis is vital for its overall function and, most

369   importantly, to promote proper spermatogenesis. Oxidative stress and a lowered antioxidant

370   capacity are hallmarks of tIRI and are the bases of its pathophysiological consequences, among

371   other factors (Turner and Lysiak, 2008; Al-Maghrebi, Kehinde and Anim, 2010). In our study,

372   the decline in glycolytic flux during tIRI was accompanied by increased testicular oxidative

373   stress as indicated by the low levels of NADPH, GSH, CAT and SOD. Under physiological

374   conditions, it is thought that proliferating cells using aerobic glycolysis are naturally protected

375   against OS due to the production of NADPH and GSH, which are natural antioxidant side

376   products of the PPP (Kuehne et al., 2015). Thus, increased ROS production as a result of tIRI

377   would disrupt the function of the enzymes and components of the metabolic and energy

378   producing pathways in germ cells. A strong association was reported between increased ROS

379   generation, abnormal semen parameters and male infertility (Ko, Sabangeh and Agarwal, 2014).

380   Recently, it was also reported that increased ROS levels in the serum and seminal fluid of

381   infertile men negatively affected sperm mitochondrial respiration through the uncoupling of

382   electron transport and ATP production (Ferramosca et al., 2013). Although considered non

383   proliferative, SCs are characterized by a high glycolytic flux and are known as lactate producers

384   due to their unique "Warburg-like metabolism" to support the continuous progression of

385   spermatogenesis (Oliveira et al., 2015). This property indirectly renders SCs insensitive to

386   physiological oxidative stress but not that induced by continuous external stimuli. Therefore,

387   ROS can be considered a regulator of glycolytic flux in proliferative germ cells and non-

388   proliferative SCs.

389   Oxygen supply insufficiency induced by ischemia or hypoxia also alters mitochondrial

390   respiratory chain function, inhibits mitochondrial ATP synthase and subsequently reduces

391   oxidative phosphorylation (Eales, Hollinshead, & Tennant, 2016). Here, we demonstrated that

392   testicular ATP levels are compromised in tIRI-subjected rats and were preserved after FBP

393   treatment. Tissue reperfusion and the restoration of oxygen supply generate ROS, open

394   mitochondrial pores and disrupt the proton balance, exacerbating ischemic injury and leading to

395   ATP depletion (Baines, 2010; Halestrap, 2010). The beneficial effects of FBP in maintaining the

396   intracellular ATP pool can occur at different levels. FBP is known to activate membrane Na^+/K^+

397   ATPase by increasing intracellular Na^+ and sustaining ionic equilibrium (Roig, Bartrons &

398   Bermudez, 1997), to stimulate PFK activity (Farias et al., 1986) and to act as an energy source

399   by stimulating anaerobic ATP production (Bickler & Buck, 1996). In the hypothermic heart, FBP

400   protection was related to the increased production of intracellular glycolytic energy (Hua et al.,

401   2003). Physiologically, each FBP molecule can produce four ATP molecules instead of two

402   ATPs produced by glucose under aerobic conditions by bypassing the first two ATP-consuming

403   reactions. Therefore, it can be hypothesized that during tIRI, the availability of FBP prior to the

404   onset of reperfusion could have rescued the cell from the decline in the HK and PFK activities

405   that require ATP and acted as a glycolytic substrate for the next ATP-generating glycolytic

406   reactions.

407   The role of p53 in regulating spermatogenesis is commonly accepted (Almon et al., 1993)

408   because its knockout in mice leads to more undifferentiated spermatogonia compared with wild-

409   type mice (Beumer et al., 1998). However, little is known about the p53 regulation of glycolytic

410   flux in testicular cells. Here, we show that tIRI-induced p53 overexpression was associated with

411   increased TIGAR expression, p53 phosphorylation, upregulation of PUMA (apoptosis inducer),

412   and downregulation of survivin (inhibitor of apoptosis), all of which were abolished by FBP

413   treatment. The fate of the cell is determined by p53 in two directions: survival and death

414   (Montero et al., 2013). Physiological levels of ROS trigger protective pathways, whereas p53

415   acts as a death signal under cytotoxic oxidative stress. It was reported that most p53-induced

416   apoptosis events are dependent on PUMA, a proapoptotic BCL-2 family protein (Jeffers et al.,

417   2003). The role of p53 in regulating carbohydrate metabolism was suggested by inducing its

418   downstream gene, TIGAR (Green and Chipuk, 2006). Under oxidative stress, p53-induced

419   TIGAR expression modulates the glycolytic pathway by lowering the levels of fructose 2,6-

420   bisphosphate, inhibiting glycolysis, and activating the PPP to protect against ROS-induced death

421   (Bensaad et al., 2006). However, under severe IRI, continued TIGAR expression could lead to

422   glycolysis shutdown and inhibition of ATP production with or without PPP activation (Bensaad,

423   Cheung and Vousden, 2009). A TIGAR-null mutation in mice was found to aggravate brain

424   ischemic injury and was associated with low NADPH and GSH levels (Li et al., 2014). In the

425   heart, p53 and TIGAR were also found to enhance hypoxia-induced inhibition of glycolysis and

426   myocyte apoptosis (Kimata et al., 2010). In mild renal IRI, p53-induced TIGAR expression

427   resulted in the inhibition of PFK1 and increased G6PD and NADPH levels, indicating the

428   redirection of the glycolytic pathway to the PPP (Kim, Devalaraja-Narashimha, & Padanilam,

429   2015). However, under severe renal IRI, sustained TIGAR expression did not activate the PPP,

430   and p53 overexpression led to cell apoptosis (Kim, Devalaraja-Narashimha, & Padanilam, 2015).

431   The results from this study suggest that tIRI-induced oxidative stress is toxic to the testicular

432   microenvironment, prompting apoptotic pathway activation through p53 overexpression and

433   phosphorylation and preventing additional global tissue damage. The inhibition of glycolysis

434   without activation of the PPP suggests that during tIRI, sustained TIGAR overexpression might

435   redirect glucose metabolism from energy production to nucleotide synthesis for DNA repair.

436

437   **Conclusion**

438   In conclusion, alterations in the mRNA expression and activities of the major GEs appear to

439   contribute to the tIRI-induced damage to spermatogenesis and hamper cellular energetics. The

440   effects of FBP treatment were very beneficial in sustaining the ATP and antioxidant levels that

441   were depleted by tIRI-induced excessive ROS production and glycolysis shutdown. In addition,

442   the activation of p53 and its transcriptional target TIGAR during tIRI was clearly associated with

443   germ cell apoptosis and did not promote their survival. These findings show promise for FBP

444   application as an adjuvant treatment in the setting of TTD.

445

446

447

448

449

450

451

452

453

454

455

456

457

458

459

460

461

462

463

464

465

REFERENCES

Ahn SM, Yoon HY, Lee BG, Park KC, Chung JH, Moon CH, Lee SH. 2002. Fructose-1,6-
diphosphate attenuates prostaglandin E2 production and cyclo-oxygenase-2 expression in
UVB-irradiated HaCaT keratinocytes. *British Journal of Pharmacology* **137**:497-503.

Al-Maghrebi M, Kehinde EO, Anim JT. 2010. Long term testicular ischemia-reperfusion
injury-induced apoptosis: involvement of survivin down-regulation. *Biochemical Biophysical
Research Communications* **395**:342-347.

Al-Maghrebi M, Renno WM, Al-Ajmi N. 2012. Epigallocatechin-3-gallate inhibits apoptosis
and protects testicular seminiferous tubules from ischemia/reperfusion-induced
inflammation. *Biochemical Biophysical Research Communications* **420**: 434-439.

Almon E, Goldfinger N, Kapon A, Schwartz D, Levine AJ, Rotter V. 1993. Testicular tissue-
specific expression of the p53 suppressor gene. *Developmental Biology* **156**:107-116.

Alves MG, Dias TR, Silva BM, Oliveira PF. **2014.** Metabolic cooperation in testis as a
pharmacological target: from disease to contraception. *Current Molecular Pharmacology*
7:83-95.

481 **Alves MG, Jesus TT, Sousa M, Goldberg E, Silva BM, Oliveira PF. 2016b.** Male fertility

482   and obesity: are ghrelin, leptin and glucagon-like peptide-1 pharmacologically relevant?

483   *Current Pharmaceutical Design* **22**:783-791.

484 **Alves MG, Martins AD, Jarak I, Barros A, Silva J, Sousa M, Oliveira PF. 2016a.** Testicular

485   lactate content is compromised in men with Klinefelter Syndrome. *Molecular Reproduction*

486   *and Development* **83**:208-216.

487 **Alves MG, Martins AD, Moreira PI, Carvalho RA, Sousa M, Barros A, Silva J, Pinto S,**

488   **Simões T, Oliveira PF. 2015.** Metabolic fingerprints in testicular biopsies from type 1

489   diabetic patients. *Cell and Tissue Research* **362**:431-440.

490 **Alves MG, Rato L, Carvalho RA, Moreira PI, Socorro S, Oliveira PF. 2013.** Hormonal

491   control of Sertoli cell metabolism regulates spermatogenesis. *Cellular and Molecular Life*

492   *Sciences* **70**:777-793.

493 **Antonuccio P, Minutoli L, Romeo C, Nicòtina PA, Bitto A, Arena S, Altavilla D, Zuccarello**

494   **B, Polito F, Squadrito F. 2006.** Lipid peroxidation activates mitogen-activated protein

495   kinases in testicular ischemia-reperfusion injury. *Journal of Urology* **176**:1666–1672.

496 **Baines CP. 2010.** The cardiac mitochondrion: nexus of stress. *Annual Reviews of Physiology*

497   **72**:61–80.

498 **Bensaad K, Cheung EC and Vousden KH. 2009.** Modulation of intracellular ROS levels by

499   TIGAR controls autophagy. *EMBO Journal* **28**:3015–3026.

500 **Bensaad K, Tsuruta A, Selak MA, Vidal MN, Nakano K, Bartrons R, Gottlieb E, Vousden**

501   **KH. 2006.** TIGAR, a p53-inducible regulator of glycolysis and apoptosis. *Cell* **126**: 107–

502   120.

503 **Ben-Yosef O, Boxer P, Ross B. 1996.** Assessment of the role of the glutathione and pentose

504   phosphate pathways in the protection of primary cerebrocortical cultures from oxidative

505   stress. *Journal of Neurochemistry* **66**:2329-2337.

506 **Berg JM, Tymoczko JL, Stryer L. 2002.** Biochemistry. New York: W H Freeman. Available at

507   http://www.ncbi.nlm.nih.gov/books/NBK22395/

508 **Beumer TL, Roepers-Gajadien HL, Gademan IS, van Buul PP, Gil-Gomez G, Rutgers DH,**

509   **de Rooij DG. 1998.** The role of the tumor suppressor p53 in spermatogenesis. *Cell Death*

510   *and Differentiation* **5**:669-677.

511 **Bickler PE, Buck LT. 1996.** Effects of fructose-1,6-bisphosphate on glutamate release and ATP

512   loss from rat brain slices during hypoxia. *Journal of Neurochemistry* **67**:1463-1468.

513 **Boussouar F, Benahmed M. 2004.** Lactate and energy metabolism in male germ cells. *Trends*

514   *in Endocrinol and Met*abolism **15**:345-350.

515 **Danshina PV, Geyer CB, Dai Q, Goulding EH, Willis WD, Kitto GB, McCarrey JR, Eddy**

516   **EM, O'Brien DA. 2010.** Phosphoglycerate kinase 2 (PGK2) is essential for sperm function

517   and male fertility in mice. Biology of Reproduction **82**:136-145.

518 **Didlake R, Kirchner KA, Lewin J, Bower JD, Markov AK. 1989.** Attenuation of ischemic

519   renal injury with fructose 1,6-diphosphate. *The journal of surgical research* **47**:220–226.

520 **Eales KL, Hollinshead KE, Tennant DA. 2016.** Hypoxia and metabolic adaptation of cancer

521   cells. *Oncogenesis* **5**:e1901-e1908.

522 **Espanol MT, Litt L, Hasegawa K, Chang LH, Macdonald JM, Gregory G, James TL, Chan**

523   **PH. 1999.** Fructose-1,6-bisphosphate preserves adenosine triphosphate but not intracellular

524   pH during hypoxia in respiring neonatal rat brain slices. *Anesthesiology* **88**:461-472.

525 **Farias LA, Smith EE, Markov AK. 1990.** Prevention of ischemichypoxic brain injury and

526   death in rabbits with fructose-1,6-diphosphate. *Stroke* **21**:606–613.

527 **Farias LA, Willis M, Gregory GA. 1986.** Effects of fructose 1,6-diphosphate, glucose, and

528   saline on cardiac resuscitation. *Anesthesiology* **65**:595–601.

529 **Ferramosca A, Conte A, Moscatelli N, Zara V. 2016.** A high fat diet negatively affects

530   rat sperm mitochondrial respiration. *Andrology*. **In press.**

531 **Ferramosca A, Pinto Provenzano S, Montagna DD, Coppola L, Zara V. 2013.** Oxidative

532   stress negatively affects human sperm mitochondrial respiration. *Urology* **82:**78-83.

533 **Filho DW, Torres MA, Bordin AL, Crezcynski-Pasa TB, Boveris A. 2004.** Spermatic cord

534   torsion, reactive oxygen and nitrogen species and ischemia-reperfusion injury. *Molecular*

535   *Aspects of Medicine* **25**:199–210.

536 **Goodson SG, Qiu Y, Sutton KA, Xie G, Jia W, O'Brien DA. 2012**. Metabolic substrates

537   exhibit differential effects on functional parameters of mouse sperm capacitation. *Biology of*

538   *Reproduction* **87**:7501-7515.

539 **Gupta GS. 2013.** Isoenzymes of glycolytic pathway in sperm: The unique sites for

540   contraception. *International Journal of Bioassays* **2**:1354-1374.

541 **Halestrap AP. 2010.** A pore way to die: the role of mitochondria in reperfusion injury and

542   cardioprotection. *Biochemical Society Transactions* **38**:841–860.

543 **Hua D, Zhuang X, Ye J, Wilson D, Chiang B, Chien S. 2003.** Using fructose-1,6-diphosphate

544   during hypothermic rabbit-heart preservation: a high-energy phosphate study. *Journal of*

545   *Heart and Lung Transplantation* **22**:574–582.

546 **Johnsen SG. 1970**. Testicular biopsy score count – a method for registration of spermatogenesis

547   in human testes: normal values and results of 335 hypogonadal males. *Hormones* **1**: 2–25.

548 **Kamp G, Schmidt H, Stypa H, Feiden S, Mahling C, Wegener G. 2007.** Regulatory

549   properties of 6-phosphofructokinase and control of glycolysis in boar spermatozoa.

550   *Reproduction* **133**:29-40.

551 **Kanwar U, Chadha S, Batla A, Sanyal SN, Sandhu R. 1988.** Effect of selected metal ions on

552   the motility and carbohydrate metabolism of ejaculated human spermatozoa. *Indian Journal*

553   *of Physiology and Pharmacology* **32**:195-201.

554 **Karaca M, Kilic E, Yazici B, Demir S, de L. 2002.** Ischemic stroke in elderly patients treated

555   with a free radical scavenger-glycolytic intermediate solution: a preliminary pilot trial.

556   *Neurological research* **24**:73–80.

557 **Katib A. 2015.** Mechanisms linking obesity to male infertility. *Central European Journal of*

558   *Urology* **68**:79-85.

559 **Kelleher JA, Chan PH, Chan TYY, Gregory GA. 1995.** Energy metabolism in hypoxic

560   astrocytes: protective mechanism of fructose-1,6-bisphosphate. *Neurochemistry research*

561   **20**:785-792.

562 **Kim J, Devalaraja-Narashimha K, Padanilam BJ. 2015.** TIGAR regulates glycolysis in

563   ischemic kidney proximal tubules. *American Journal of Physiology. Renal Physiology*

564   **308**:F298-308.

565 **Kimata M, Matoba S, Iwai-Kanai E, Nakamura H, Hoshino A, Nakaoka M, Katamura M,**

566   **Okawa Y, Mita Y, Okigaki M, Ikeda K, Tatsumi T, Matsubara H. 2010.**

567   p53 and TIGAR regulate cardiac myocyte energy homeostasis under hypoxic stress.

568   *American Journal of Physiology. Heart and Circulation Physiology* **299**:H1908-H1916.

569 **Krisfalusi M, Miki K, Magyar PL, O'Brien DA. 2006.** Multiple glycolytic enzymes are tightly

570   bound to the fibrous sheath of mouse spermatozoa. *Biology of Reproduction* **75**:270–278.

571   **Ko EY, Sabanegh ES, Jr., Agarwal A. 2014.** Male infertility testing: Reactive oxygen species

572   and antioxidant capacity. *Fertility and Sterility* **102**:1518-1527.

573   **Kuehne A, Emmert H, Soehle J, Winnefeld M, Fischer F, Wenck H, Gallinat S, Terstegen**

574   **L, Lucius R, Hildebrand J, Zamboni N. 2015.** Acute Activation of Oxidative Pentose

575   Phosphate Pathway as First-Line Response to Oxidative Stress in Human Skin Cells.

576   *Molecular Cell* **59**:359-371.

577   **Li M, Sun M, Cao L, Gu JH, Ge J, Chen J, Han R, Qin YY, Zhou ZP, Ding Y, Qin ZH.**

578   **2014.** A TIGAR-regulated metabolic pathway is critical for protection of brain ischemia.

579   *Journal of Neuroscience* **34**:7458-7471.

580   **Livak KJ, Schmittgen TD. 2001.** Analysis of relative gene expression data using realtime

581   quantitative PCR and the 2(_Delta Delta C(T)) Method. *Methods* **25**:402–408.

582   **Martins AD, Moreira AC, Sá R, Monteiro MP, Sousa M, Carvalho RA, Silva BM, Oliveira**

583   **PF, Alves MG. 2015**. Leptin modulates human Sertoli cells acetate production and

584   glycolytic profile: a novel mechanism of obesity-induced male infertility? *Biochimica et*

585   *Biophysica Acta* **1852**:1824-1832.

586   **Miki, K. 2007.** Energy metabolism and sperm function. Soc. *Reproduction and Fertility*

587   *Supplement* **65**:309-325.

588   **Miki K, Qu W, Goulding EH, Willis WD, Bunch DO, Strader LF, Perreault SD, Eddy EM,**

589   **O'Brien DA. 2004.** Glyceraldehyde 3-phosphate dehydrogenase-S, a sperm-specific

590   glycolytic enzyme, is required for sperm motility and male fertility. *Proceedings of the*

591   *National Academy of Science USA* **101**:16501-16506.

592   **Minutoli L, Bitto A, Squadrito F, Irrera N, Rinaldi M, Nicotina PA, Arena S, Magno C,**

593   **Marini H, Spaccapelo L, Ottani A, Giuliani D, Romeo C, Guarini S, Antonuccio P,**

594   **Altavilla D. 2011.** Melanocortin 4 receptor activation protects against testicular ischemia-

595   reperfusion injury by triggering the cholinergic antiinflammatory pathway. *Endocrinology*.

596   **152**:3852-3861.

597   **Montero J, Dutta C, van Bodegom D, Weinstock D, Letai A. 2013.** p53 regulates a non-

598   apoptotic death induced by ROS. *Cell Death and Differentiation* **20**:1465-1474.

599   **Mukai C, Okuno M. 2004.** Glycolysis plays a major role for adenosine triphosphate

600   supplementation in mouse sperm flagellar movement. *Biology of Reproduction* **71**:540-547.

601   **Nakamura N, Mori C, Eddy EM. 2010.** Molecular complex of three testis-specific isozymes

602   associated with the mouse sperm fibrous sheath: hexokinase 1, phosphofructokinase M, and

603   glutathione S-transferase mu class 5. *Biology of Reproduction* **82**:504-515.

604   **Odet F, Gabel S, London RE, Goldberg E, Eddy EM. 2013.** Glycolysis and mitochondrial

605   respiration in mouse LDHC-null sperm. *Biology of Reproduction* **88**:95,1-7.

606   **Oliveira PF, Martins AD, Moreira AC, Cheng CY, Alves MG. 2015.** The Warburg effect

607   revisited—lesson from the Sertoli cell. *Medicinal Research Reviews* **35**:126-151.

608   **Planas ME, Sánchez S, González P, Rodrigues de Oliveira J, Bartrons R. 1993.** Protective

609   effect of fructose 1,6-bisphosphate against carrageenan-induced inflammation. *European*

610   *Journal of Pharmacology* **237**:251-255.

611   **Rato L, Alves MG, Cavaco JE, Oliveira PF. 2014.** High-energy diets: a threat for male

612   fertility? *Obesity Reviews* **15**:996-1007.

613   **Rato L, Alves MG, Dias TR, Lopes G, Cavaco JE, Socorro S, Oliveira PF. 2013.** High-

614   energy diets may induce a pre-diabetic state altering testicular glycolytic metabolic profile

615   and male reproductive parameters. *Andrology* **1**:495-504.

616 **Rato L, Alves MG, Duarte AI, Santos MS, Moreira PI, Cavaco JE, Oliveira PF. 2015.**

617 Testosterone deficiency induced by progressive stages of diabetes mellitus impairs glucose

618 metabolism and favors glycogenesis in mature rat Sertoli cells. *The International Journal of*

619 *Biochemistry and Cell Biology* **66**:1-10.

620 **Rato L, Alves MG, Socorro S, Duarte AI, Cavaco JE, Oliveira PF. 2012.** Metabolic

621 regulation is important for spermatogenesis. *Nature Reviews Urology* **9**:330-338.

622 **Riera MF, Meroni SB, Schteingart HF, Pellizzari EH, Cigorraga SB. 2002.** Regulation of

623 lactate production and glucose transport as well as of glucose transporter 1 and lactate

624 dehydrogenase A mRNA levels by basic fibroblast growth factor in rat Sertoli cells. *Journal*

625 *of Endocrinology* **173**:335–343.

626 **Robinson R, Fritz IB. 1981.** Metabolism of glucose by Sertoli cells in culture. *Biology of*

627 *Reproduction* **24**:1032–1041.

628 **Roig, T., Bartrons, R., Bermudez, J. 1997.** Exogenous fructose-1,6-diphosphate reduces K^+

629 permeability in isolated rat hepatocytes. *American Journal of Physiology* **273**:C473–C478.

630 **Salvemini F, Franzé A, Iervolino A, Filosa S, Salzano S, Ursini MV. 1999.** Enhanced

631 glutathione levels and oxidoresistance mediated by increased glucose-6-phosphate

632 dehydrogenase expression. *Journal of Biological Chemistry* **274**:2750-2757.

633 **Tanii I, Yagura T, Inagaki N, Nakayama T, Imaizumi K, Yoshinaga K. 2007.** Preferential

634 localization of rat GAPDS on the ribs of fibrous sheath of sperm flagellum and its expression

635 during flagellar formation. Acta Histochemica et Cytochemica **40**:19-26.

636 **Travis AJ, Tutuncu L, Jorgez CJ, Ord TS, Jones BH, Kopf GS, Williams CJ. 2004.**

637 Requirements for glucose beyond sperm capacitation during in vitro fertilization in the

638 mouse. *Biology of Reproduction* **71**:139-145.

639 **Turner TT, Lysiak JJ. 2008.** Oxidative stress: a common factor in testicular dysfunction.

640 *Journal of Andrology* **29**:488-498.

641 **Williams AC, Ford WC. 2001.** The role of glucose in supporting motility and capacitation in

642 human spermatozoa. *Journal of Andrology* **22**:680-695.

643 **Zhou J, Wang F, Zhang J, Gao H, Yang Y, Fu R. 2014.** Repeated febrile convulsions impair

644 hippocampal neurons and cause synaptic damage in immature rats: neuroprotective effect of

645 fructose-1,6-diphosphate. *Neural Regeneration Research* **9**:937-942.

646

647

648

649

650

651

652

653

654

655

1

Figure 1 Histological analysis of testicular tissue.

H & E sections of rat ipsilateral testes showing low (A, B and C; 10×) and high (D, E and F; 40×) magnifications of the histological changes from the three experimental groups. (A and D) Representative images of ipsilateral testes from the sham group showing a normal seminiferous tubule structure and normal germ cell layer arrangement. (B and E) Histological sections of ipsilateral testes from the tIRI group showing seminiferous tubule atrophy and disrupted germ cell layers. (C and F) Examples of histological findings of the FBP-treated group (2 mg/kg i.p.) showing preserved histological morphology of the seminiferous tubules.
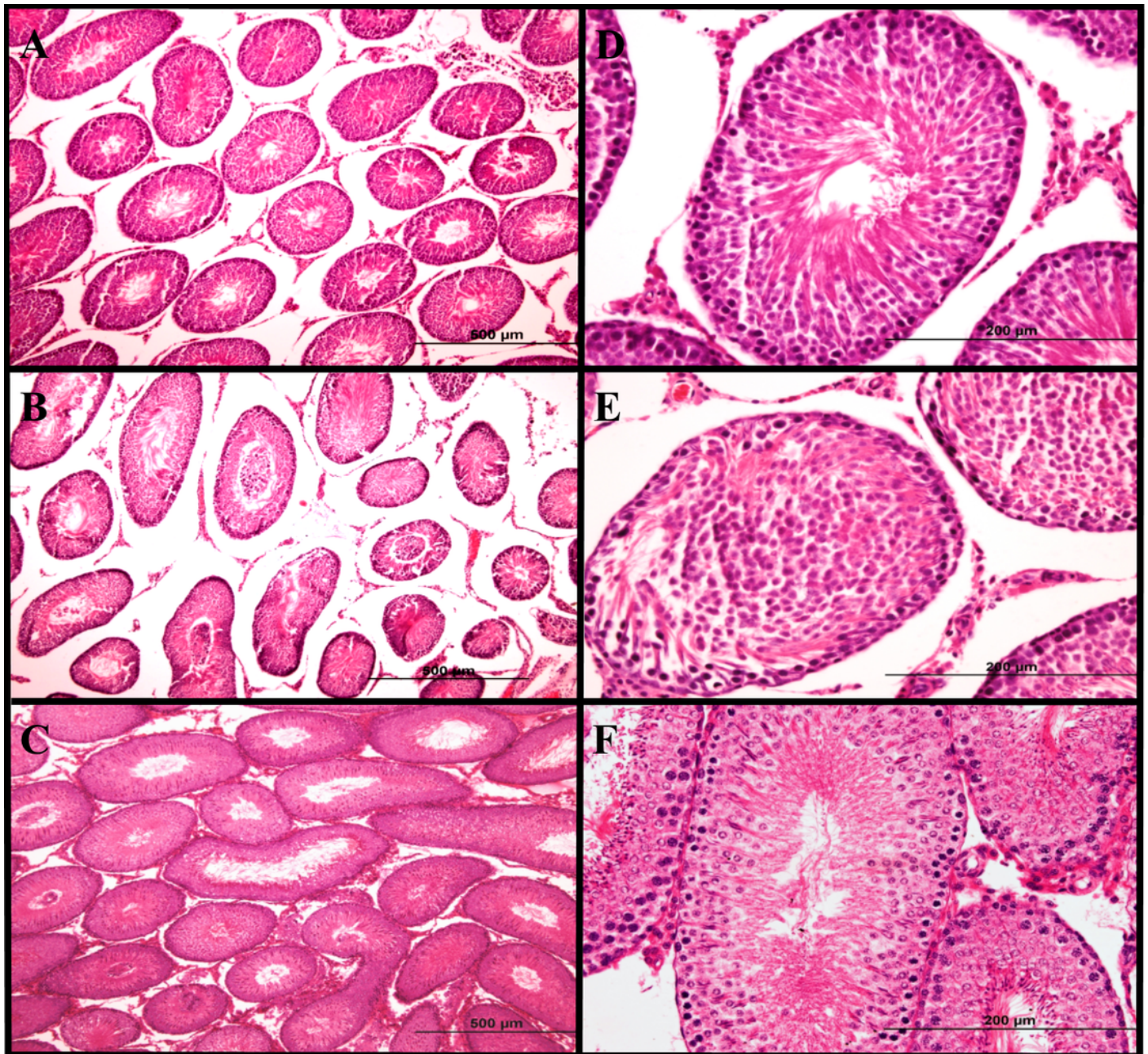
2

Figure 2 FBP effects on ATP and NADPH levels.

(A) tIRI-induced ATP depletion ($^*p$ = 0.0087) was preserved in the FBP-treated group ($^\#p$ = 0.0286). (B) The tIRI-induced decrease in NADPH levels ($^*p$ = 0.0004) was alleviated by FBP treatment ($^\#p$ = 0.0168). Data analysis was performed using one-way analysis of variance (ANOVA) followed by the Holm-Sidak multiple comparisons test. Data are presented as the mean ± SD (n = 6). The significance of the data is indicated with * compared with the sham group and $^\#$ compared with the tIRI group.
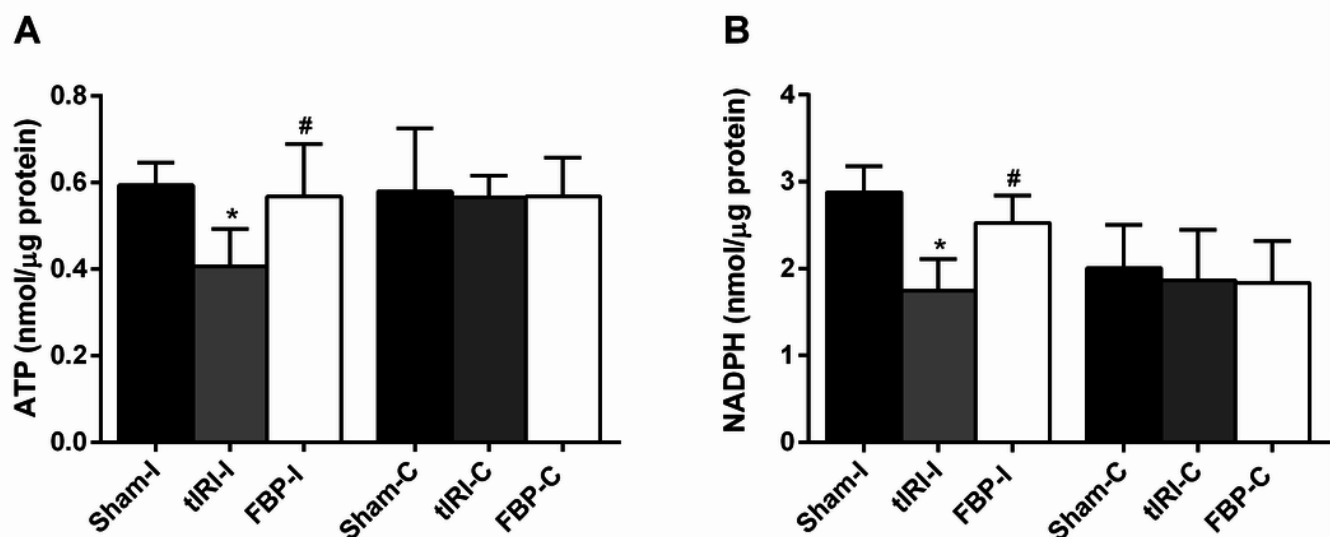
Figure 3 Germ cell apoptosis (GCA) assessed by TUNEL immunohistofluorescence.

(A, D, and G) Representative images of GCA in sham rats. (B, E, and H) Increased number of TUNEL-positive nuclei in the tIRI group. (C, F, and I) FBP-treated group showing a diminished number of TUNEL-positive nuclei. Fluorescence staining used in the images: A, D, and G = TUNEL; B, E, and H = DAPI, and C, F, and I = Merged.

*Note: Auto Gamma Correction was used for the image. This only affects the reviewing manuscript. See original source image if needed for review.
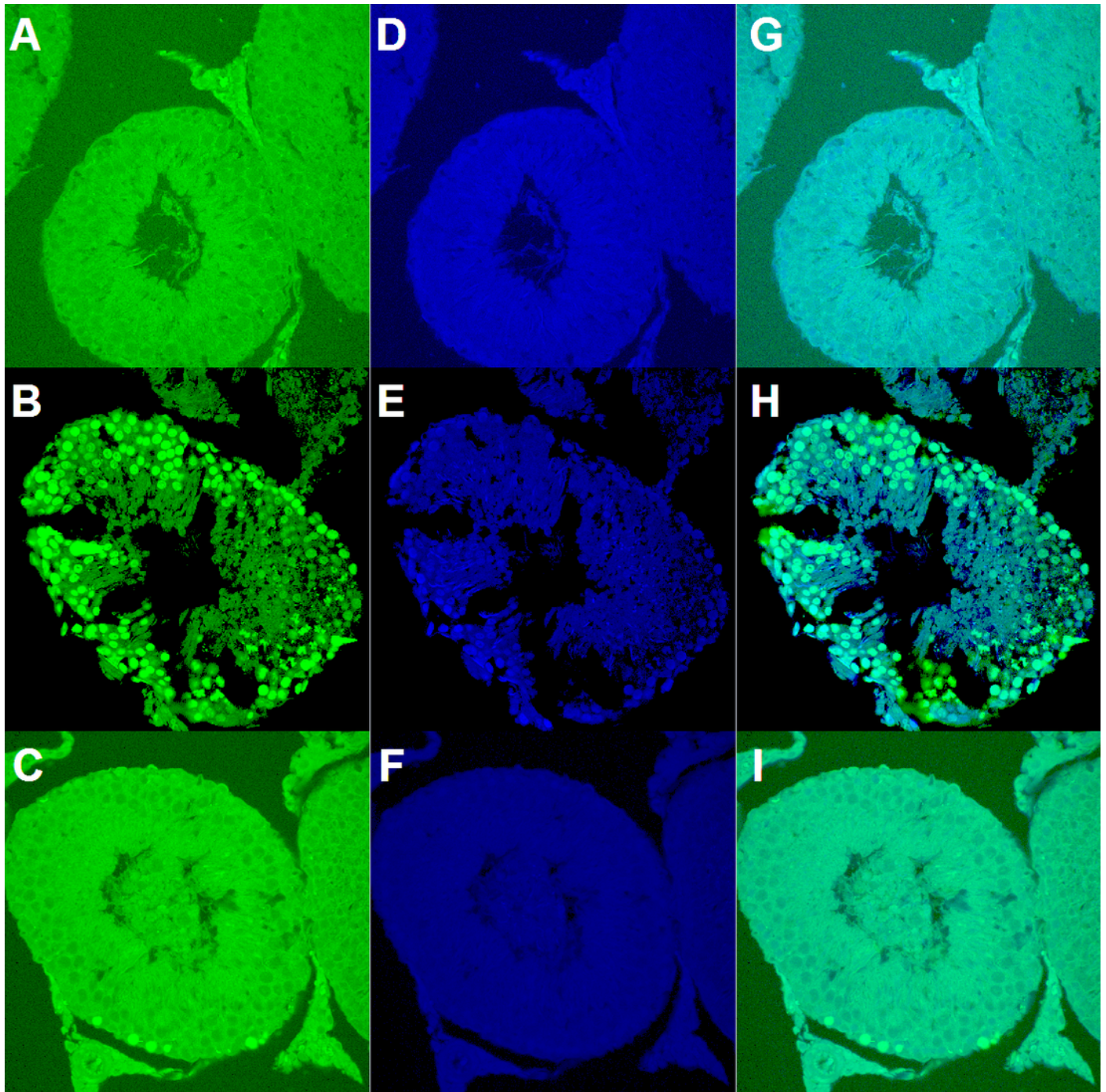
4

Figure 4 Phosphorylation of p53 and modulation of its downstream genes.

(A) Increased p53 phosphorylation (ser 15) was induced by tIRI (*p < 0.0001) and was inhibited by FBP treatment (#p < 0.0001). Real-time PCR was used to measure the relative mRNA expression of (B) PUMA and (C) survivin. PUMA mRNA levels were increased during tIRI (*p < 0.05), whereas survivin mRNA was decreased (*p < 0.05). FBP treatment normalized the relative mRNA expression of PUMA (#p < 0.05) and survivin (#p < 0.05). Data analysis was performed using one-way analysis of variance (ANOVA) followed by the Holm-Sidak multiple comparisons test. Data are presented as the mean ± SD (n = 6). The significance of the data is indicated with * compared with the sham group and # compared with the tIRI group.
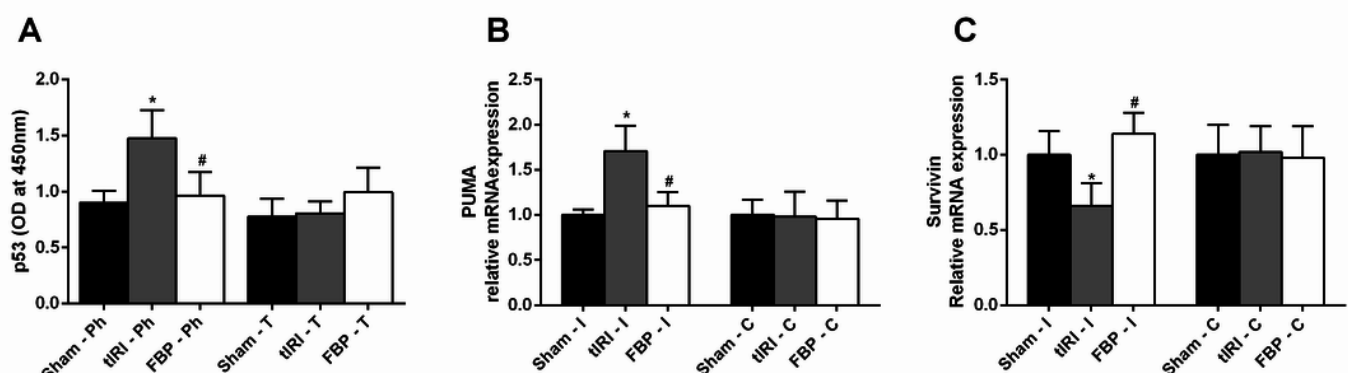
5

Figure 5 Immunoexpression of p53 and TIGAR in paraffin-embedded ipsilateral testicular tissue.

(A and D) The sham group showing very weak immunostaining of the p53 and TIGAR antibodies, respectively, in the seminiferous tubules layers of the rat testes. (B and E) Examples of p53 and TIGAR immunostaining showing a notable increase in their immunoexpression after tIRI. (C and F) FBP treatment of tIRI-subjected rats showed a decrease in the p53 and TIGAR immunolabeling intensity in the testes compared with the tIRI group. Magnification = 40×.
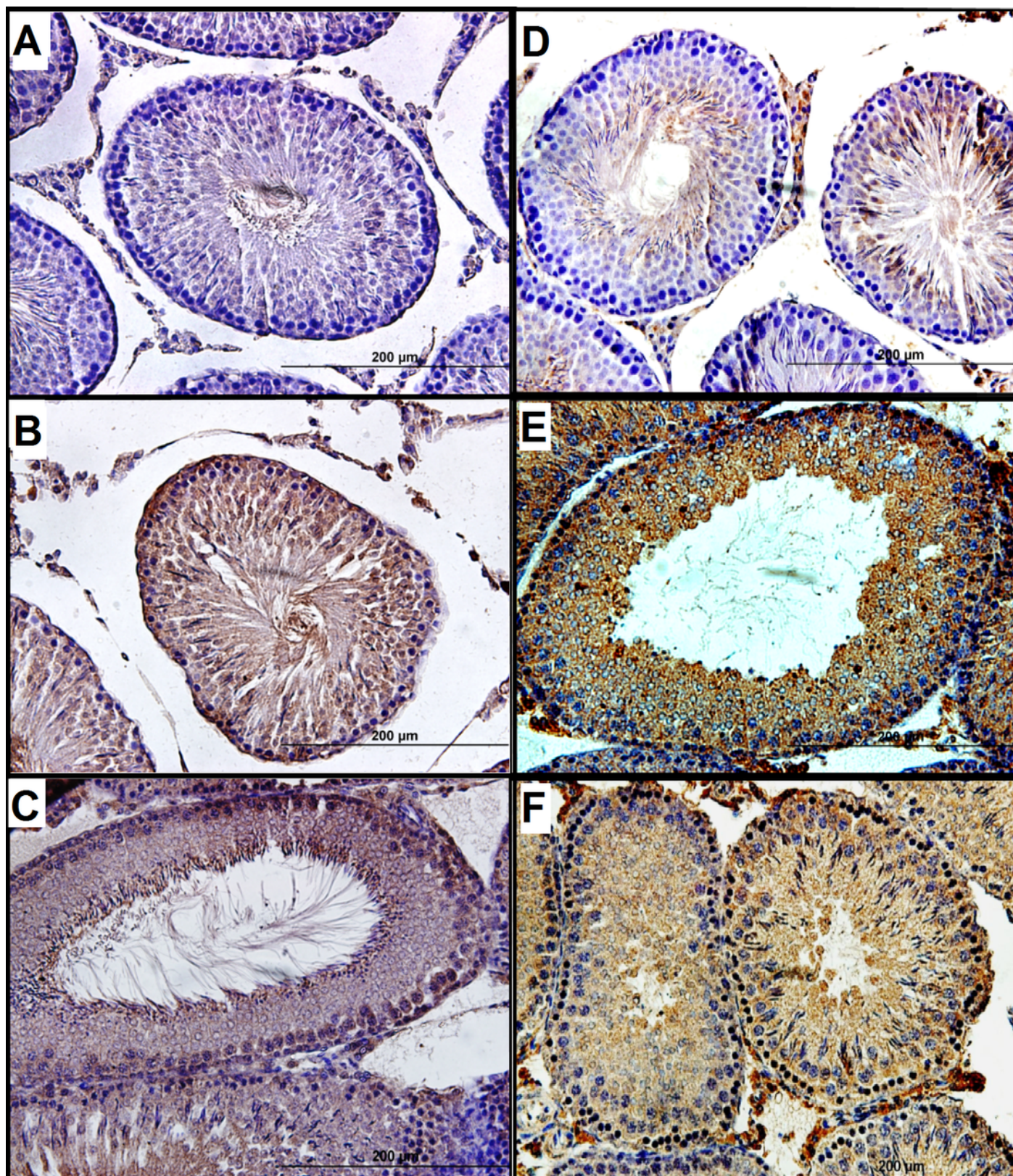
Relative mRNA expression [RQ ($2^{-\Delta\Delta CT}$)] of glycolytic enzymes

			RQ ($2^{-\Delta\Delta CT}$)	
Gene Name		**Sham**	**tIRI**	**FBP**
Hk1	I	1.00 ± 0.26	$0.76 \pm 0.46^*$	$1.06 \pm 0.49^\#$
	C	1.00 ± 0.09	1.05 ± 0.33	1.13 ± 0.26
Gpi	I	1.00 ± 0.31	0.91 ± 0.64	0.93 ± 0.45
	C	1.00 ± 0.22	1.13 ± 0.33	1.00 ± 0.54
Pfk1	I	1.00 ± 0.27	$0.66 \pm 0.39^*$	$0.91 \pm 0.21^\#$
	C	1.00 ± 0.39	1.10 ± 0.59	1.19 ± 0.28
Gapdhs	I	1.00 ± 0.32	$0.73 \pm 0.39^*$	$0.92 \pm 0.30^\#$
	C	1.00 ± 0.07	1.02 ± 0.09	1.05 ± 0.10
Pgk2	I	1.00 ± 0.24	1.05 ± 0.55	1.19 ± 0.35
	C	1.00 ± 0.22	0.92 ± 0.24	1.09 ± 0.50
Ldhc	I	1.00 ± 0.26	$0.76 \pm 0.46^*$	$1.06 \pm 0.46^\#$
	C	1.00 ± 0.09	1.05 ± 0.33	1.14 ± 0.26
Actin, beta	I	-	-	-
	C	-	-	-

Notes.

[1]Rats received an i.p. injection of FBP (2 mg/kg) 30 min prior to reperfusion.

Data analysis was determined by the one way analysis of variance (ANOVA)

accompanied by the Holms-Sidak multiple comparisons test. Data are presented

as mean $\pm$ SD (n = 6).

2   * tIRI compared to sham; # FBP compared to tIRI.

3   I ipsilateral; C contralateral.

Activities of glycolytic enzymes

		Sham	tIRI	p value[*]	FBP[1]	p value[#]
HK1	I	2.08 ± 0.30	1.11 ± 0.27	0.0034	1.87 ± 0.38	0.0260
	C	1.72 ± 0.43	1.71 ± 0.48	ns	1.55 ± 0.70	ns
GPI	I	0.91 ± 0.11	0.77 ± 0.12	0.2046	0.71 ± 0.16	0.8686
	C	0.73 ± 0.14	0.88 ± 0.10	ns	0.79 ± 0.09	ns
PFK1	I	1.33 ± 0.24	0.78 ± 0.10	0.016	1.30 ± 0.17	0.0029
	C	1.2 ± 0.21	1.08 ± 0.30	ns	1.42 ± 0.25	ns
GAPDHS	I	1.49 ± 0.14	1.05 ± 0.21	0.0016	1.46 ± 0.28	0.0040
	C	1.36 ± 0.15	1.32 ± 0.18	ns	1.37 ± 0.16	ns
PGK2	I	0.98 ± 0.21	0.77 ± 0.09	0.1388	0.81 ± 0.14	0.9894
	C	0.92 ± 0.19	0.84 ± 0.15	ns	0.83 ± 0.17	ns
LDHC	I	2.02 ± 0.41	1.07 ± 0.17	< 0.0001	1.78 ± 0.19	0.0017
	C	2.02 ± 0.34	2.02 ± 0.16	ns	1.84 ± 0.43	ns

Notes.

[1]Rats received an i.p. injection of FBP (2 mg/kg) 30 min prior to reperfusion.

Enzyme activities are expressed in milliunits/µg protein and data are presented as mean $\pm$ SD (n = 6).

Data analysis was determined by the one way analysis of variance (ANOVA) accompanied by the Holms-Sidak multiple comparisons test.

[*] tIRI compared to sham; [#] FBP compared to tIRI.

I ipsilateral; C contralateral.

Levels of oxidative stress markers

		Sham	tIRI	*p* value*	FBP[1]	*p* value#
GSH	I	0.25 ± 0.04	0.33 ± 0.03	0.0002	0.23 ± 0.01	<0.0001
	C	0.22 ± 0.02	0.21 ± 0.02	ns	0.19 ± 0.01	ns
MDA	I	1.05 ± 0.20	1.68 ± 0.35	< 0.0001	1.04 ± 0.25	< 0.0001
	C	1.03 ± 0.07	0.98 ± 0.06	ns	1.01 ± 0.08	ns
SOD	I	95.67 ± 3.59	81.23 ± 0.95	< 0.0001	92.62 ± 1.87	0.0004
	C	94.12 ± 2.48	92.03 ± 3.52	ns	90.53 ± 7.23	ns
CAT	I	95.32 ± 3.91	82.55 ± 8.52	0.0002	94.75 ± 4.10	0.0003
	C	94.07 ± 4.17	92.32 ± 3.19	ns	97.09 ± 0.98	ns

Notes.

[1]Rats received an i.p. injection of FBP (2 mg/kg) 30 min prior to reperfusion.

Parameter units: GSH (nmol/μg); MDA (μM); SOD (inhibition rate %); and CAT (units/ml).

Data analysis was determined by the one way analysis of variance (ANOVA) accompanied by

the Holms-Sidak multiple comparisons test. Data are presented as mean $\pm$ SD (n = 6).

* tIRI compared to sham; # FBP compared to tIRI.

I ipsilateral; C contralateral.